

## A DFT study on direct benzene hydroxylation catalyzed by framework Fe and Al sites in zeolites†

Cite this: *Catal. Sci. Technol.*, 2014, 4, 2490

Received 24th March 2014,  
Accepted 23rd April 2014

DOI: 10.1039/c4cy00369a

www.rsc.org/catalysis

Gang Yang<sup>\*ab</sup> and Lijun Zhou<sup>a</sup>

Three-coordinated framework Fe sites in zeolites were theoretically demonstrated to show Lewis acidity and superior catalytic activity for the titled reaction compared with extra-framework Fe sites that were generally considered as the active species, while the corresponding Al sites are not reactive. This catalytic distinctness is ascribed to their divergent  $\alpha$ -oxygen structures.

Owing to peculiar adsorption and catalytic properties, isomorphous incorporation and cation exchange in zeolites have recently been given significant attention.<sup>1</sup> Zeolites modified with iron show pronounced activity for the selective oxidation of benzene to phenol.<sup>2–4</sup> It is generally believed that the catalytic performance of these materials stems from the high reactivity of extra-framework iron sites stabilized in zeolite micropores.<sup>2,3,5–9</sup> The exact structure of these species is still under debate.<sup>7,10</sup>

Notwithstanding, zeolites with framework Fe sites were also detected to show catalytic activity for the above mentioned reaction.<sup>11–15</sup> At a given Fe content, zeolites synthesized with framework Fe sites are significantly more catalytically active than those only with cation exchange (extra-framework Fe).<sup>11,14</sup> This is an indication that the framework Fe sites are also involved in the catalysis. The tetrahedral framework Fe sites with Brønsted acidity (Fig. 1a) are known to be catalytically inactive for the selective benzene oxidation reaction.<sup>14,16</sup> This

drives us to speculate that the superior catalytic activity is caused by three-coordinated framework Fe sites (Fig. 1b) resulting from pretreatment with steam or at high temperatures in He.

In fact, the three-coordinated Al sites in zeolites, that are kept in the framework, have been observed experimentally after similar pretreatments,<sup>17,18</sup> and the amount of three-coordinated Al sites increases with the elevation of the pretreatment temperatures. These Al species show Lewis acidity and catalytic activity for a variety of chemical reactions,<sup>18–20</sup> and the Fe analogue is assumed to have similar Lewis acidity and catalytic properties. Here, density functional calculations were employed with the aim to demonstrate the Lewis acidity of the [Fe]-ZSM-5 zeolite and the catalytic activity for the selective oxidation of benzene. The Lewis acidity and catalytic performance of the [Al]-ZSM-5 zeolite were also explored, and no similar catalytic properties have been detected. The catalytic distinctness of the three-coordinated framework Al and Fe sites was then clarified.

The tetrahedral framework Al and Fe sites in zeolites ( $M_B$ , Fig. 1a) are found to have consistent structures with previously calculated and experimental results. For the three-coordinated framework Al and Fe sites ( $M_L$ , Fig. 1b), the M atoms and three neighbouring O atoms interact more

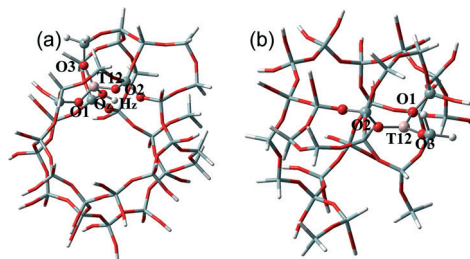


Fig. 1 The Brønsted (a) and Lewis (b) acidic sites in [M]-ZSM-5 zeolites (M = Al, Fe), where the metal centers are tetrahedrally ( $M_B$ ) and three ( $M_L$ ) coordinated, respectively.

<sup>a</sup> College of Resources and Environment & Chongqing Key Laboratory of Soil Multi-scale Interfacial Process, Southwest University, 400715, Chongqing, China. E-mail: theobiochem@gmail.com

<sup>b</sup> Engineering Research Center of Forest Bio-preparation, Ministry of Education, Northeast Forestry University, 150040 Harbin, China

† Electronic supplementary information (ESI) available: Computational methods (S1), configurational distortions (S2), O<sub>3</sub> decomposition (S3), stability of the  $\alpha$ -oxygen species (S4) and figures of N<sub>2</sub>O adsorption on the Lewis Brønsted and acidic sites as well as benzene adsorption on the  $\alpha$ -oxygen site of the framework Al Lewis acidic site. See DOI: 10.1039/c4cy00369a

strongly than in the case of the tetrahedral sites resulting in shorter M–O distances (Table S1†). The Al configuration in the Al<sub>L</sub> deviates from the planar triangle by 11.71°, this is probably due to the strain force exhibited by the associated zeolite frameworks. As a result of the larger M–O bond distances, a larger configurational distortion from a planar triangle is observed for the Fe center in the Fe<sub>L</sub>, see the ESI† (S2). The three-coordinated Al sites, whether at the framework or extra-framework, are known to show Lewis acidity resulting mainly from the non-bonding 3p<sub>z</sub> orbital.<sup>17</sup> The lowest-unoccupied molecular orbital (LUMO) that is often used to characterize Lewis acidity predominates at the Al center, see Fig. 2a.

For the three-coordinated framework Fe sites (Fe<sub>L</sub>), the LUMO is principally localized at the Fe center (Fig. 2b) and resembles the scenario of the Al<sub>L</sub>. The presence of Lewis acidity in the Fe<sub>L</sub> is due to the fact that the non-bonding 3d orbitals of the Fe center are good electron acceptors, the same as the Ti centers in zeolites.<sup>21,22</sup> As a matter of fact, FeCl<sub>3</sub> has been widely used as a Lewis acid catalyst.<sup>23</sup> The LUMO energies, that should be used cautiously for different metal centers,<sup>24,25</sup> are respectively calculated at –0.035 and –0.026 eV for the Fe<sub>L</sub> and the Al<sub>L</sub>, implying comparable Lewis acid strengths. This is supported by close N<sub>2</sub>O adsorption energies (–13.8 and –16.9 kcal mol<sup>–1</sup> on the Fe<sub>L</sub> and the Al<sub>L</sub>, respectively). In both adsorption cases, direct bonds form between the metal centers and N<sub>2</sub>O, see Fig. S3†. The O4–N1 bonds (bond orders) in the Al<sub>L</sub> and the Fe<sub>L</sub> are equal to 1.226 (1.362) and 1.218 (1.412) Å, respectively. These values show slight elongations compared to the gas-phase, 1.195 Å (1.543), and resemble the scenarios of N<sub>2</sub>O adsorption onto extra-framework Fe sites<sup>5,8–10,26</sup> and framework Al Lewis acidic sites.<sup>19</sup> In contrast, N<sub>2</sub>O shows very weak H-bonding interactions with tetrahedral framework Al and Fe sites and the O4–N1 and N1–N2 bonds remain almost intact (Fig. S4†).

The reaction mechanisms for N<sub>2</sub>O decomposition and benzene hydroxylation on the Fe Lewis acidic site are proposed on the basis of DFT-calculated results, see Scheme 1. The reaction is initiated by N<sub>2</sub>O adsorption (step 1, 1 → 2), followed by decomposition (step 2, 2 → 3) *via* the first transition state (TS1). Then the weakly interacting N<sub>2</sub> detaches and the α-oxygen site (4) is realised and is ready for subsequent catalysis. To our surprise, the approach of benzene to the α-oxygen site (step 4, 4 → 5) results in the direct formation of the O4–C1 bond without an energy barrier. This is distinct from the extra-framework Fe sites where this step has a high-

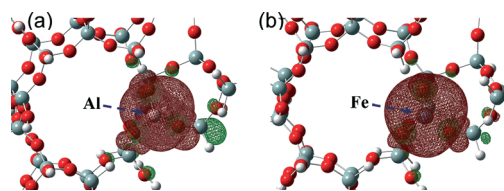
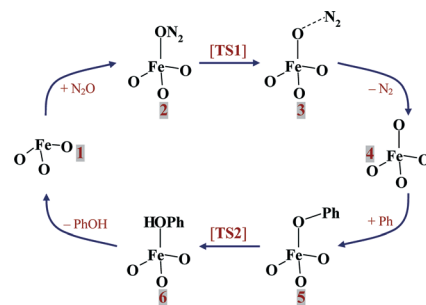


Fig. 2 The lowest-unoccupied molecular orbitals (LUMOs) of the Lewis acidic sites in [Al]-ZSM-5 (a) and [Fe]-ZSM-5 (b) zeolites.



Scheme 1 The catalytic cycle of N<sub>2</sub>O decomposition and benzene hydroxylation over the Lewis acidic site of the [Fe]-ZSM-5 zeolite.

energy transition state.<sup>5,8–10,26</sup> Then phenol is produced as a result of an intra-molecular proton transfer from C1 to O1 (step 5, 5 → 6), and the reaction is completed by desorption of phenol.

As Fig. 3 indicates, the energy barrier for N<sub>2</sub>O decomposition (step 2) equals 49.9 kcal mol<sup>–1</sup> and exceeds that of the extra-framework Fe sites.<sup>5,8–10,26</sup> With the use of 5-T cluster models, an energy barrier of 44.6 kcal mol<sup>–1</sup> has been predicted for the extra-framework mononuclear-Fe site,<sup>5</sup> and similar computational methodologies as in this work obtain a barrier of 33.7 kcal mol<sup>–1</sup>.<sup>26</sup> This suggests that the α-oxygen site is more likely to produce extra-framework Fe sites, and then migrate to framework Fe Lewis acidic sites and catalyze the benzene hydroxylation reaction. As shown in the ESI† (S3), α-oxygen species of the Fe Lewis acidic site can also be readily obtained by alternative oxidants such as O<sub>3</sub>.

It has been indicated above that the adsorption of benzene onto the α-oxygen results in the formation of the O4–C1 bond in a barrier-less manner (step 4), and this greatly facilitates the benzene hydroxylation process in contrast to an appreciable activation energy barrier for the extra-framework Fe sites.<sup>8,9,26,27</sup> The superior catalytic activity of the framework

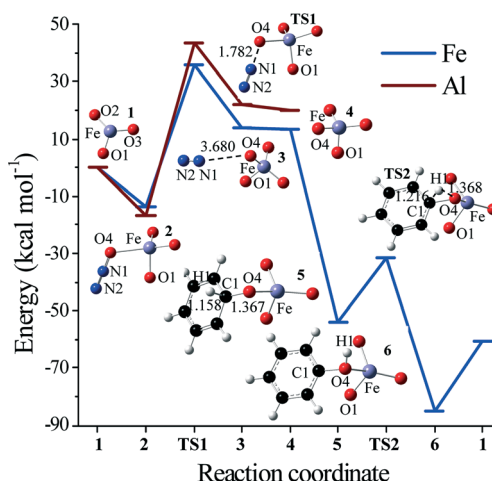


Fig. 3 The ONIOM(M06L:B3LYP) energy diagrams of N<sub>2</sub>O decomposition and benzene hydroxylation reactions over the framework Lewis acidic sites of [M]-ZSM-5 zeolites (M = Fe, Al) as well as the local structures of the energy minima and transition states for the Fe Lewis acidic site. Selected distances are given in Å.

Fe site is probably due to the lower stability of its  $\alpha$ -oxygen species, see more details in the ESI† (S4). The following step (5  $\rightarrow$  6) is an intra-molecular proton transfer that requires an energy barrier of 21.7 kcal mol<sup>-1</sup>, close to that of the extra-framework Fe sites.<sup>20</sup> The benzene hydroxylation reaction over the framework Fe Lewis acidic site is preferred to that over the extra-framework Fe sites, both thermodynamically and kinetically (Fig. 3). Thus, it has been demonstrated that after steaming or high-temperature pretreatment in He, zeolites synthesized with framework Fe sites are more catalytically active than those only with ion exchange.<sup>11,14</sup>

Now we will discuss the catalytic activity of the framework Al Lewis acidic site (Al<sub>L</sub>). It is assumed that N<sub>2</sub>O on the Al<sub>L</sub> decomposes in a way resembling that of the Fe<sub>L</sub>, shown in Fig. 3. The energy barrier of the reaction with the Al<sub>L</sub> equals 60.5 kcal mol<sup>-1</sup> and hence N<sub>2</sub>O decomposition becomes implausible under normal conditions; furthermore, there are no extra-framework Fe sites in Al-substituted zeolites for assistance. Notwithstanding, benzene hydroxylation has been considered for the Al<sub>L</sub>, and the adsorption of benzene on the  $\alpha$ -oxygen site does not result in the formation of the C1–O4 bond, see Fig. S5.† Instead, all of the benzene C atoms have long bond lengths with the  $\alpha$ -oxygen site; e.g., C1–O4: 4.543 Å. This differs significantly from the scenario of the framework Fe Lewis acidic site. Due to weak interactions, the adsorbed benzene remains almost intact, as in the gas phase, and the C–C and C–H bond distances are altered by no more than 0.003 Å. This evidence shows that the presence of Fe sites is indispensable for the catalysis of the benzene hydroxylation reaction, which is consistent with experimental observations.<sup>28,29</sup>

The distinct catalytic properties of framework Al and Fe Lewis acidic sites may be caused by the structural discrepancy of their  $\alpha$ -oxygen sites, see Fig. 4. The  $\alpha$ -oxygen species (O4) of the Al<sub>L</sub> (4-Al<sub>L</sub>) forms a direct bond with the framework-O1 atom, with a distance (bond order) of 1.551 Å (0.945). As indicated in Table 1, O4 and O1 atoms constitute the peroxide (O<sub>2</sub><sup>2-</sup>) species, which in the absence of metal ions seems unable to activate the hydrocarbon C–H bonds.<sup>30</sup> On the contrary, the  $\alpha$ -oxygen species (O4) in the [Fe]–ZSM-5 zeolite (4-Fe<sub>L</sub>) does not form chemical bonds with the framework-O atoms and features the anion radical (O<sup>-</sup>, Table 1 and Fig. 4).<sup>31</sup> This means that the Fe–O<sup>-</sup> species has been created over the framework Fe Lewis acidic site, which has been postulated for extra-framework Fe sites and shows good

**Table 1** Selected distances (*r*), Mulliken charges (*q*) and spin densities (*s*) for the Lewis acidic (M<sub>L</sub>) and  $\alpha$ -oxygen (4-M<sub>L</sub>) sites in [M]–ZSM-5 zeolites (M = Al, Fe) as well as H<sub>2</sub>O<sub>2</sub><sup>a</sup>

	4-Al <sub>L</sub>	4-Fe <sub>L</sub>	Al <sub>L</sub>	Fe <sub>L</sub>	H <sub>2</sub> O <sub>2</sub>
<i>r</i> (O1–O4)/Å	1.551	2.546			1.467
<i>q</i> (O1)	–0.387	–0.635	–0.611	–0.720	–0.274
<i>q</i> (O4)	–0.309	–0.303			–0.274
<i>q</i> (M)	1.057	1.230	1.029	1.235	
<i>s</i> (O1)		0.321		0.260	
<i>s</i> (O4)		1.036			
<i>s</i> (M)		3.224		4.182	

<sup>a</sup> Calculated at the ONIOM(M06L:B3LYP)//B3LYP level.

catalytic performance for benzene hydroxylation<sup>31</sup> and ethylene epoxidation<sup>32</sup> reactions.

In summary, we have theoretically explored the Lewis acidity of three-coordinated framework Al and Fe sites in zeolites and, for the first time, their catalytic activity for the benzene hydroxylation reaction. It is assumed that the  $\alpha$ -oxygen species develop at the extra-framework Fe sites and then migrate to framework Fe Lewis acidic sites or are generated by alternative oxidants. The  $\alpha$ -oxygen species corresponding to framework Fe Lewis acidity shows unique catalytic activity for the benzene hydroxylation reaction, thus satisfactorily explaining the experimental result that zeolites synthesized with framework Fe sites have superior catalytic activity compared to those with only ion exchange. On the contrary, framework Al Lewis sites are not catalytically active for this reaction and the catalytic distinctness of the Fe sites is ascribed to the structural divergence of their  $\alpha$ -oxygen sites. The  $\alpha$ -oxygen species of the framework Fe Lewis acidity features the Fe–O<sup>-</sup> species that has been proposed to form over extra-framework Fe sites.

The National Natural Science Foundation (no. 20903019) and Fundamental Research Funds for the Central Colleges (SWU113049 and XDJK2014C106) are acknowledged for their financial support. E. A. Pidko (Eindhoven University of Technology) is greatly thanked for helpful discussions. Shanghai Supercomputing Center and National Supercomputing Center in Shenzhen are acknowledged for offering the computational resources.

## Notes and references

- J. B. Nagy, R. Aiello, G. Giordano, A. Katovic, F. Testa, Z. Kónya and I. I. Kiricsi, *Molecular sieves*, ed. H. G. Karge and J. Weitkamp, Springer, Berlin/Heidelberg, 2007, vol. 5, pp. 365–478.
- G. I. Panov, A. K. Uriarte, M. A. Rodkin and V. I. Sobolev, *Catal. Today*, 1998, **41**, 365–385.
- K. A. Dubkov, N. S. Ovanesyan, A. A. Shteinman, E. V. Starokon and G. I. Panov, *J. Catal.*, 2002, **207**, 341–352.
- A. J. J. Koekkoek, H. C. Xin, Q. H. Yang, C. Li and E. J. M. Hensen, *Microporous Mesoporous Mater.*, 2011, **145**, 172–181.
- J. A. Ryder, A. K. Chakraborty and A. T. Bell, *J. Phys. Chem. B*, 2002, **106**, 7059–7064.

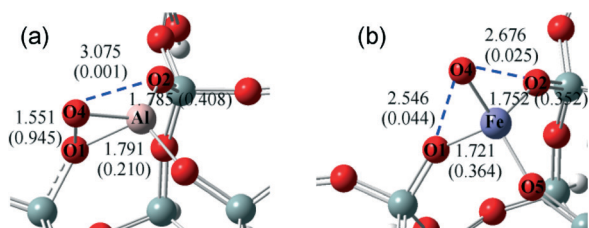


**Fig. 4** The  $\alpha$ -oxygen structures generated by N<sub>2</sub>O decomposition on the framework Al (a) and Fe (b) Lewis acidic sites. Selected distances are given in Å (bond orders in parentheses).

- 6 J. A. Ryder, A. K. Chakraborty and A. T. Bell, *J. Catal.*, 2003, **220**, 84–91.
- 7 A. Zecchina, M. Rivallan, G. Berlier, C. Lamberti and G. Ricchiardi, *Phys. Chem. Chem. Phys.*, 2007, **9**, 3483–3499.
- 8 M. F. Fellah, R. A. van Santen and I. Onal, *J. Phys. Chem. C*, 2009, **113**, 15307–15313.
- 9 G. N. Li, E. A. Pidko, R. A. van Santen, Z. C. Feng, C. Li and E. J. M. Hensen, *J. Catal.*, 2011, **284**, 194–206.
- 10 G. Yang, J. Guan, L. J. Zhou, X. C. Liu, X. W. Han and X. H. Bao, *Catal. Surv. Asia*, 2010, **14**, 85–94.
- 11 Y. F. Chang, J. G. McCarty and Y. L. Zhang, *Catal. Lett.*, 1995, **34**, 163–177.
- 12 A. Ribera, I. W. C. E. Arends, S. de Vries, J. Pérez-Ramírez and R. A. Sheldon, *J. Catal.*, 2000, **195**, 287–297.
- 13 D. Meloni, R. Monaci, V. Solinas, G. Berlier, S. Bordiga, I. Rossetti, C. Oliva and L. Forni, *J. Catal.*, 2003, **214**, 169–178.
- 14 I. Yuranov, D. A. Bulushev, A. Renken and L. Kiwi-Minsker, *J. Catal.*, 2004, **227**, 138–147.
- 15 J. K. Lee, Y. J. Kim, H. J. Lee, S. H. Kim, S. J. Cho, I. S. Nam and S. B. Hong, *J. Catal.*, 2011, **284**, 23–33.
- 16 G. I. Panov, *CATTECH*, 2000, **4**, 18–32.
- 17 J. A. van Bokhoven, A. M. J. van der Eerden and D. K. Koningsberger, *J. Am. Chem. Soc.*, 2003, **125**, 7435–7442.
- 18 C. Busco, V. Bolis and P. Ugliengo, *J. Phys. Chem. C*, 2007, **111**, 5561–5567.
- 19 R. Wischert, P. Laurent, C. Copéret, F. Delbecq and P. Sautet, *J. Am. Chem. Soc.*, 2012, **134**, 14430–14449.
- 20 S. H. Li, A. M. Zheng, Y. C. Su, H. L. Zhang, L. Chen, J. Yang, C. H. Ye and F. Deng, *J. Am. Chem. Soc.*, 2007, **129**, 11161–11171.
- 21 A. Corma and H. Garcia, *Chem. Rev.*, 2003, **103**, 4307–4366.
- 22 G. Yang, L. J. Zhou, X. C. Liu, X. W. Han and X. H. Bao, *Chem. - Eur. J.*, 2011, **17**, 1614–1621.
- 23 A. A. O. Sarhan and C. Bolm, *Chem. Soc. Rev.*, 2009, **38**, 2730–2744.
- 24 G. Sastre and A. Corma, *Chem. Phys. Lett.*, 1999, **302**, 447–453.
- 25 G. Yang, E. A. Pidko and E. J. M. Hensen, *J. Phys. Chem. C*, 2013, **117**, 3976–3986.
- 26 Z. W. Yang, G. Yang, X. C. Liu and X. W. Han, *Catal. Lett.*, 2013, **143**, 260–266.
- 27 Y. Shiota, K. Suzuki and K. Yoshizawa, *Organometallics*, 2006, **25**, 3118–3123.
- 28 P. Kuánek, B. Wichterlová and Z. Sobalík, *J. Catal.*, 2002, **211**, 109–118.
- 29 E. J. M. Hensen, Q. Zhu, R. A. J. Janssen, P. C. M. M. Magusin, P. J. Kooyman and R. A. van Santen, *J. Catal.*, 2005, **233**, 123–135.
- 30 G. Yang, J. Guan, L. J. Zhou, X. C. Liu, X. W. Han and X. H. Bao, *J. Photochem. Photobiol., A*, 2009, **202**, 122–127.
- 31 M. V. Parfenov, E. V. Starokon, S. V. Semikolenov and G. I. Panov, *J. Catal.*, 2009, **263**, 173–180.
- 32 E. V. Starokon, M. V. Parfenov, L. V. Pirutko, I. E. Soshnikov and G. I. Panov, *J. Catal.*, 2014, **309**, 453–459.